

# Approach to EUV Lithography Simulation

Atsushi Sekiguchi  
*Litho Tech Japan Corporation*  
Japan

## 1. Introduction

### 1.1 Simulation based on measured development rate measurements

EUV lithography is a reduced projection lithography technology based on 13.5 nm wavelength EUV (Extreme Ultraviolet). Development of EUV lithography is currently underway for the mass production of semiconductor devices for 90 nm design rule applications for ArF dry exposures and for 65 to 45 nm design rule applications for ArF immersion exposures [1-2]. EUV lithography is among the most promising next-generation lithography tools for the 32 nm technology node [3]. The evolving consensus is that EUV exposure technologies will be applied to mass production from the year 2011 [4]. Table 1 showed the relationship among technology node, exposure numerical aperture (NA), and process coefficient factor ( $k_1$ ) [5]. Achieving the 32 nm node based on an ArF laser source exposure technology will require the development of an optical system with NA increased to 1.55 and  $k_1$  improved to 0.26. In contrast, an exposure technology based on an EUV light source will permit the use of an optical system with 0.25 NA for mass production of the 32 nm node with room to spare. The requirement for the  $k_1$  factor is an easy-to-meet value of 0.59. These factors underscore the promise and importance of EUV exposure technologies. However, the development of EUV exposure equipment presents its own set of technology barriers, as does the development of ArF immersion exposure system. A wavelength of 13.5 nm requires a reflecting optical system with a combination of multiple multilayer reflecting mirrors [6], since no lens material can be used in the 13.5 nm wavelength range, if we rule out dioptric lenses. The development of EUV exposure equipment requires further examination of component technologies, including technologies related to light sources, illumination optical systems, projection optical systems, and masks. Although various exposure equipment manufacturers are actively promoting the development of EUV reduced projection exposure equipment [7-8], a resist material for EUV lithography must be developed before the first exposure system can be introduced. We have developed a new virtual lithography evaluation system with lithograph simulation that takes an approach completely different from conventional resist evaluation technologies (direct evaluation method), which require actual patterning to assess resists. The new evaluation system focuses on open-frame exposures using an EUV light source, measurements of development rates at various exposure doses, and lithography simulations based on development rate data. This chapter presents the results of our evaluations of EUV resists using this new system.

Wavelength (nm)	Tech. Node	65 nm	45 nm	32 nm	22 nm	16 nm
	NA	k1	k1	k1	K1	k1
193	0.93	0.31				
	1	0.4				
	1.2		0.28			
	1.35		0.31	0.22	0.15	
	1.35DP			0.20	0.18	
13.5	0.25			0.59	0.41	
	0.35				0.57	0.41
	0.45					0.53

Table 1. Relationship among technology node, numerical aperture (NA), and process factor ( $k_1$ )

**1.2 System configuration**

The virtual lithography evaluation system (VLES) proposed consists of an EUV open-frame exposure system, a resist development analyzer, and a lithography simulator. Fig. 1 is a schematic diagram of the VLES.

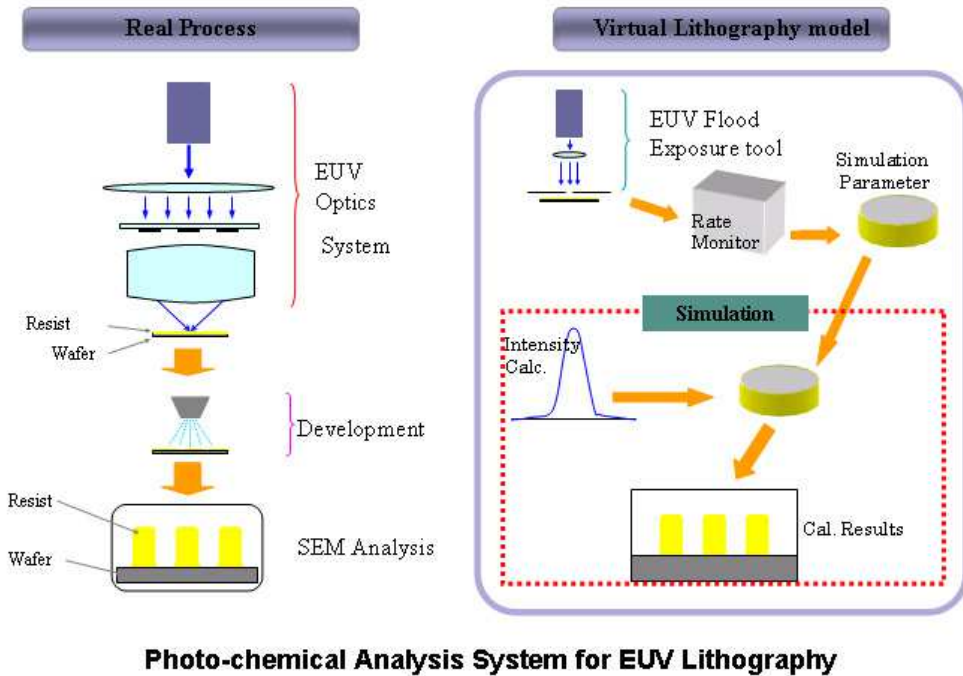


Fig. 1. Schematic diagram of the VLES

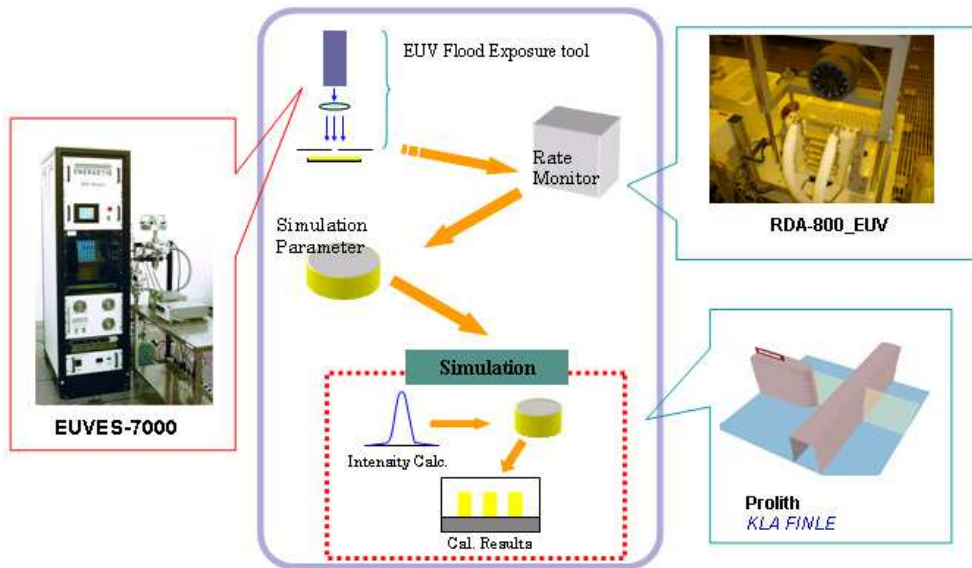


Fig. 2. Analyzers used in the VLES

Fig. 2 shows the analyzers comprising the VLES.

### 1.2.1 EUV open-frame exposure system (EUVES-7000)

This equipment uses an electrodeless Z-pinch discharge-excitation plasma light source [9] manufactured by Energetiq Technology Inc. It extracts 13.5 nm light using a Zr filter and multilayer reflecting mirrors. The exposure pattern is a 10 mm x 10 mm open frame; 12 exposures can be achieved per wafer at varying exposure doses. Fig. 3 gives an external view of this equipment and a picture of an exposure pattern (after exposure, PEB, and development).

The plasma emissions produced by the EQ-10M pass through the Zr filter to remove UV-region rays. Next, the Mo-Si multilayer reflector selectively reflects only 13.5 nm rays, which are shaped by the aperture into a 10 mm x 10 mm exposure region. The rotary Mo-Si multilayer reflector directs the light at a reflection angle of 45 degrees toward the exposure chamber at the upper section of the equipment during the exposure of a substrate. For power measurements, it rotates and directs the light to the power measurement diode chamber at the lower section of the equipment. Exposures are performed as the wafer rotates. A total of 12 exposures are possible per wafer at varying exposure doses.



(a)



(b)

Fig. 3. (a) External view of EUVES-7000 and (b) exposure pattern

Fig. 4 is a picture of the beam line.

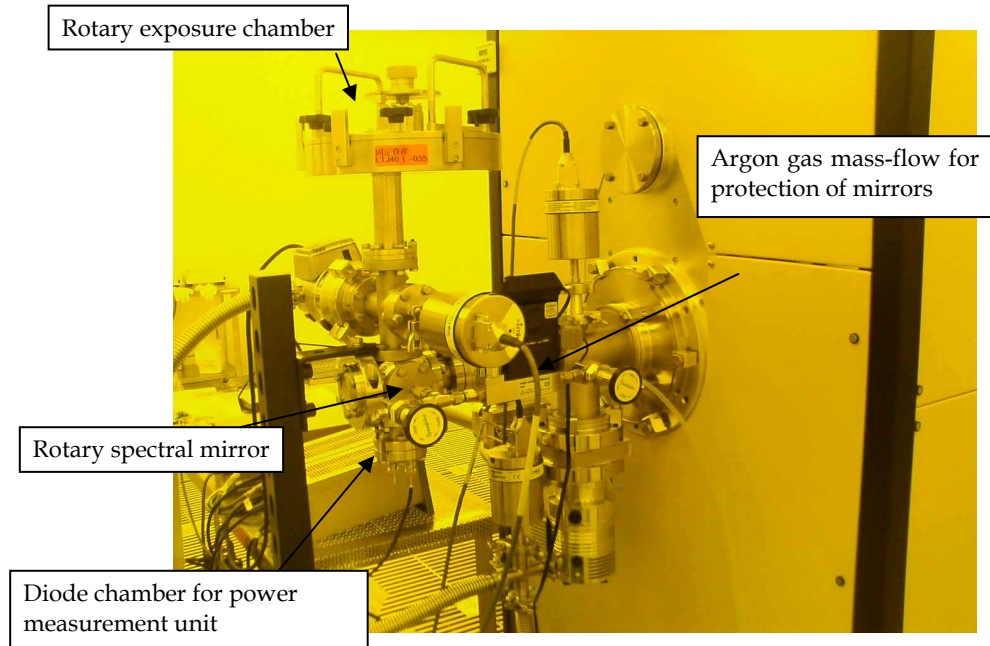


Fig. 4. Beam line for EUV exposure

### 1.2.2 Resist development analyzer (RDA-800EUV)

Following the exposure, a wafer is processed for PEB. Then, following measurement of film thickness, this resist development analyzer is used to measure the development rate of a resist corresponding to each exposure dose [10].

### 1.2.3 EUV lithography simulator (Prolith Ver. 9.3)

The obtained development rate data file is imported into the Prolith lithography simulator [11] (manufactured by KLA-Tencor) for EUV lithography simulation.

## 1.3 Experiment and results

We investigated the sensitivity of positive- and negative-type resists in EUV exposures with the system as described above, then performed simulations using the development rate data obtained.

Table 2 gives the conditions of the resists in our experiment.

The negative-type resists examined were the SAL-601 electron beam resist and SU-8 epoxy-resin-base chemically amplified resist. The positive-type resists used in our experiment were ZEP-520 non-chemically amplified electron beam resist, EUVR-1 and EUVR-2 acrylic-resin-base resists, and EUVR-3 low-molecular-weight resist.

Negative type						
Resist	Maker	Pre-bake		PEB		Thickness (nm)
		Temp. (deg.C)	Time (s)	Temp. (deg.C)	Time (s)	
SAL-601	Rohm & Hass	105	60	115	60	100
SU-8	Nippon Kayaku	90	90	95	100	100
Positive type						
Resist	Maker	Pre-bake		PEB		Thickness (nm)
		Temp. (deg.C)	Time (s)	Temp. (deg.C)	Time (s)	
ZEP-520A	Nippon Zeon	90	90	95	100	100
EUVR-1	TOK	120	90	120	90	100
EUVR-2	TOK	100	90	110	90	100
EUVR-3	TOK	110	90	100	90	100

Table 2. Conditions of resists in the experiment

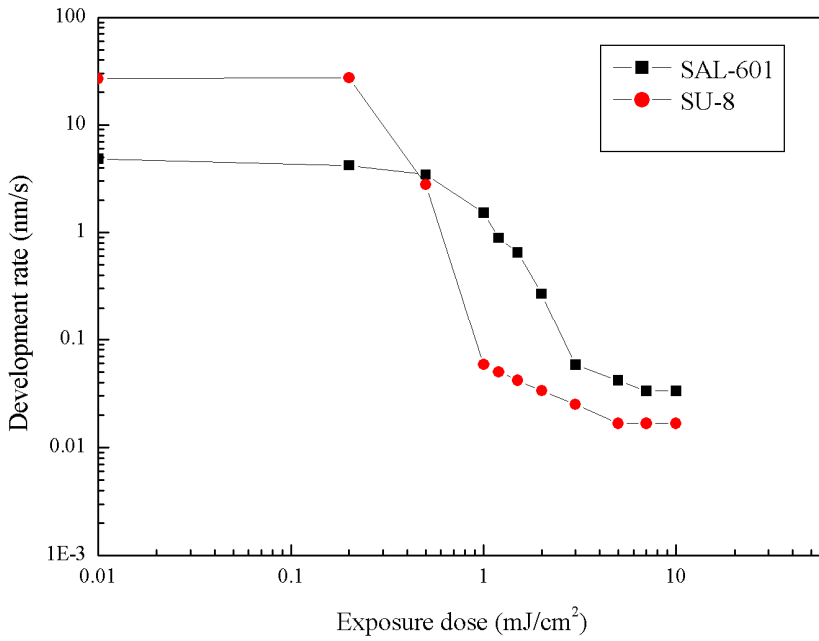
Fig. 5.(a) shows discrimination curves for negative-type resists; Fig. 5.(b) shows discrimination curves for positive-type resists.

Posi-Type	Eth(60) mJ/cm <sup>2</sup>	$\gamma_{60}$	$\tan\theta$
SAL-601	0.928	-1.445	-2.23
SU-8	0.478	-3.023	-3.73

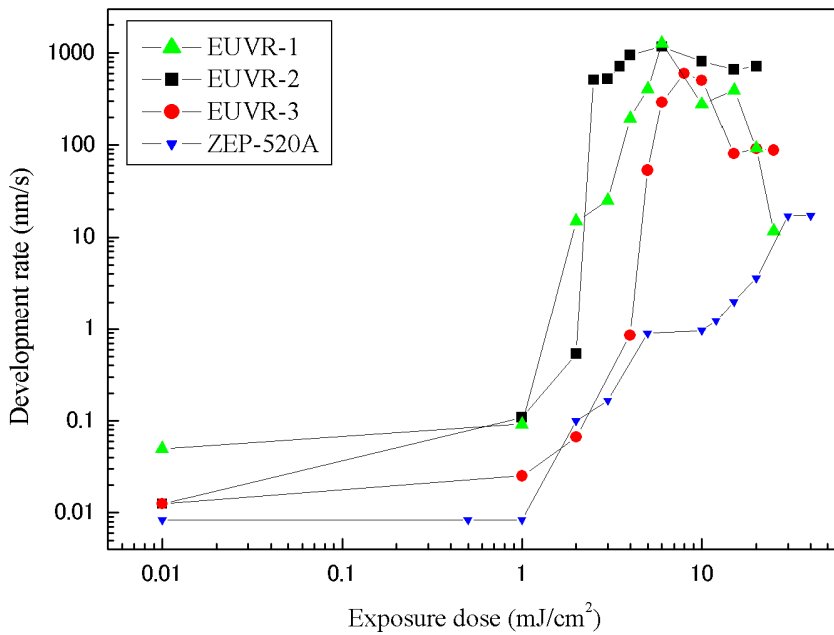
Nega-Type	Eth(60) mJ/cm <sup>2</sup>	$\gamma_{60}$	$\tan\theta$
ZEP-520A	14.710	1.669	1.90
EUVR-1	2.562	2.325	5.06
EUVR-2	8.574	3.997	30.75
EUVR-3	8.497	1.528	14.53

Table 3. Development characteristics

Table 3. shows the results of development characteristic evaluations. The results show EUVR-2 provides the highest contrast.



(a) Discrimination curves for negative-type resists



(b) Discrimination curves for positive-type resists

Fig. 5. Relationship between development rate and exposure dose

**1.4 Simulation**

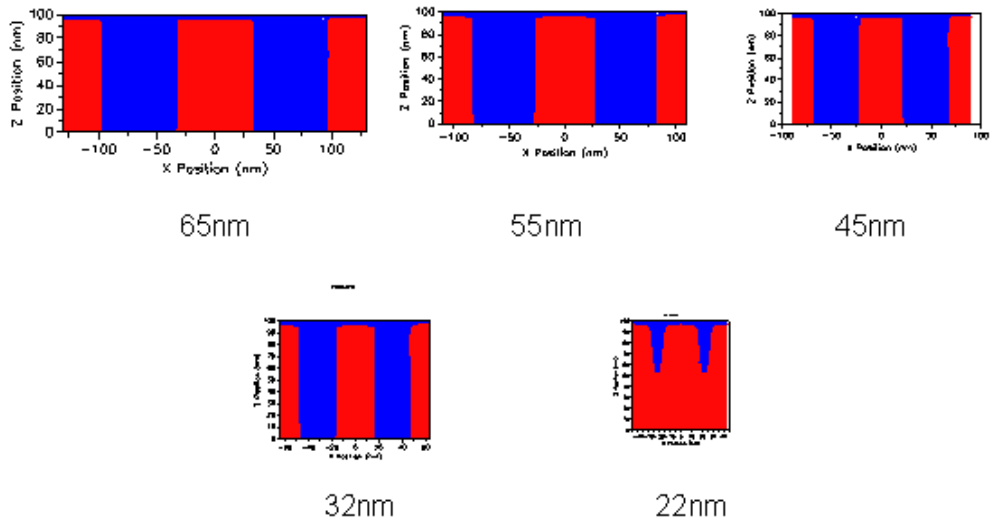
We performed a simulation using the EUV-PM2 development data. Table 4 gives the simulation conditions.

Wavelength (nm)	13.5
NA	0.3
$\sigma$	0.8
Reduction	1/5

Table 4. Simulation conditions (with Nikon HiNA-3)

We examined L&S<sup>\*1</sup> patterns and isolated patterns with pattern dimensions of 65, 55, 45, 32, and 22 nm. Defocus was examined using a 32 nm L&S pattern. Figures 6 through 8 show the simulation results. With L&S patterns, resolution can be maintained up to 32 nm. For isolated patterns, the results suggest that resolution on the order of 22 nm is within reach. In the defocus simulation, the simulation results support estimates of an attainable resolution range of -0.1 to +0.1  $\mu\text{m}$ .

\*1L&S: Line and space



L&S Pattern simulation, Exposure dose= 17.2mJ/cm<sup>2</sup>

Fig. 6. Simulation results (65-22 nm Line and space patterns)



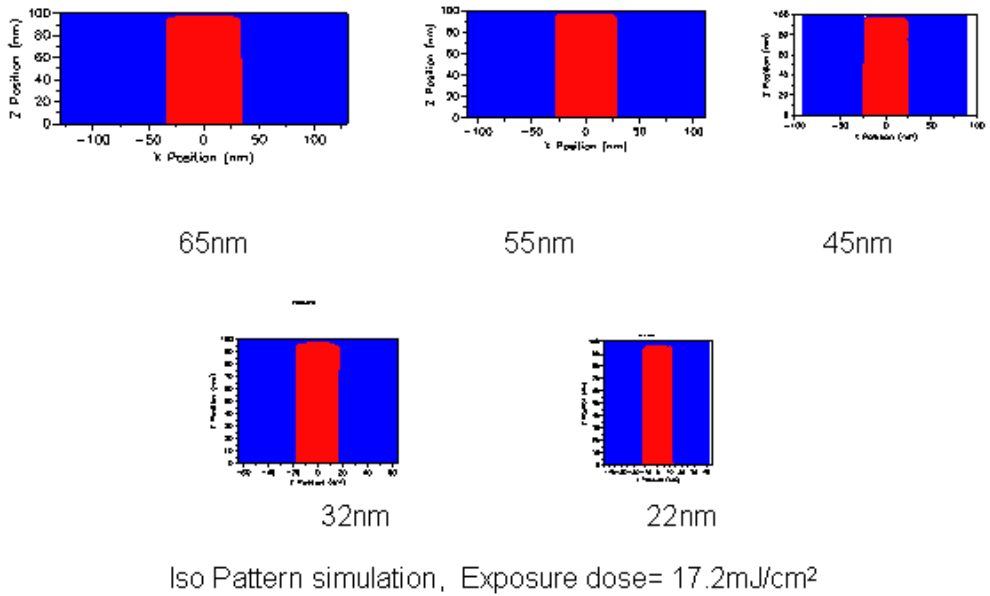
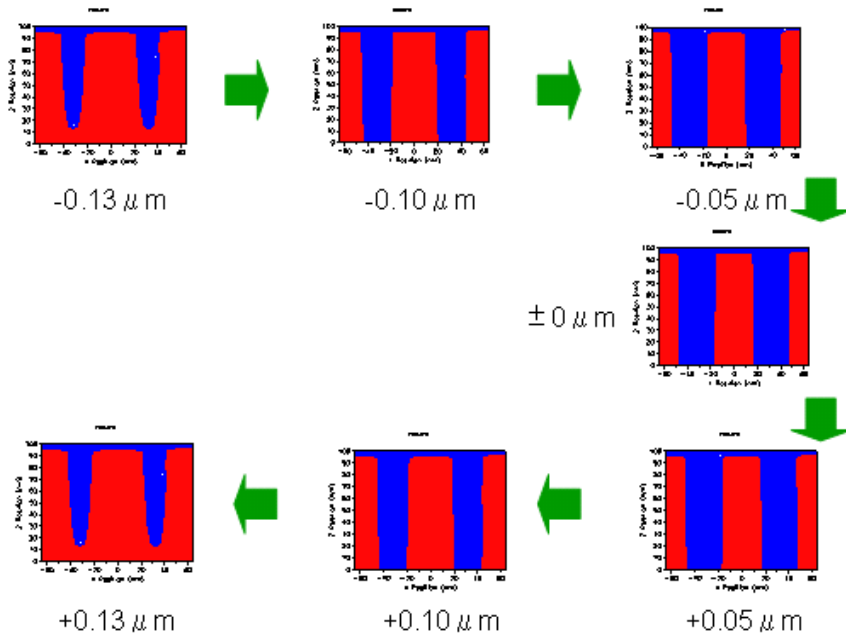


Fig. 7. Simulation results (65-22 nm Isolated patterns)



Defocus simulation / L&S=32nm /Exposure dose=17.2mJ/cm<sup>2</sup>

Fig. 8. Simulation results (32 nm L&S/defocus -0.13~+0.13 $\mu\text{m}$ )

## 1.5 Conclusion

The VLES consists of the EUVES-7000 EUV open-frame exposure system, RDA-800EUV development rate analyzer, and Prolith lithography simulator. We used the VLES to compare the sensitivity and development contrast of negative- and positive-type resists with EUV exposure. We also simulated EUV exposures using development rate data for the EUVR-2, which showed the highest development contrast of all resists tested. The results of the experiment suggest that it should be possible to obtain resolutions of 32 nm with L&S patterns and 22 nm with isolated patterns. We also calculated defocus characteristics with a 32 nm L&S pattern. Based on these calculations, we estimate a focus margin of approximately 0.2  $\mu\text{m}$  in defocus width. We believe using the system as described in this paper will permit the development of photoresist materials for EUV and expedite process development without requiring the purchase of costly EUV exposure equipment.

## 2. Simulating EUV Resists (Comparison of KrF and EUV Exposures)

### 2.1 Introduction

According to ITRS Roadmap 2007 Update Version [12], EUVL is currently the most promising candidate for 22 nm half-pitch lithography. The component technologies required for EUVL mass production must be established before the start of mass production of DRAM half-pitch, currently scheduled for 2016. RLS specifications for realizing 22 nm half-pitch resolution were presented at the 7th EUVL Symposium [13] in Lake Tahoe, California, in October 2008.

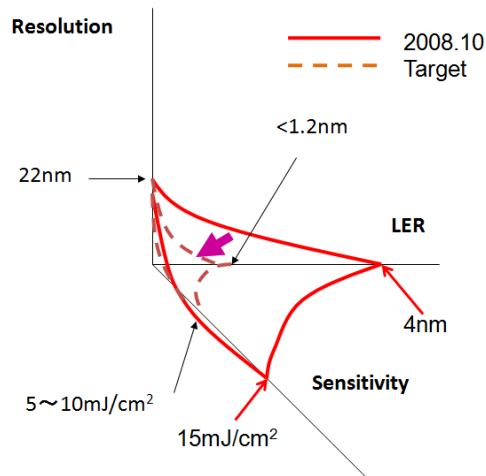


Fig. 9. RLS specifications targeting 22 nm half-pitch

A resolution of 22 nm half-pitch requires sensitivity of 5 to 10  $\text{mJ}/\text{cm}^2$  and LER of less than 1.2 nm. At an international conference, it has been pointed out that although resolutions have reached the target value, sensitivity lags, at 15  $\text{mJ}/\text{cm}^2$ , while LER (Line Edge Roughness) is no less than 4 nm. These are the best values achieved to date. Lithography simulations should prove highly effective in advancing the state of current research, given the time required to perform experiments.

The conventional EUVL simulation method involves obtaining parameters by exposing the resist to EUV. However, EUV exposure equipment is costly, and the types of exposure equipment available are limited. For these reasons, we explored the possibility of performing EUVL simulations using parameters obtained with KrF exposures. The idea was that if we detected no significant differences between parameters obtained with KrF and EUV exposures, we could use the simpler KrF exposure method to obtain valid simulation parameters for EUVL. Using EUV resists, we obtained parameters by performing both KrF and EUV exposures, then compared the parameters and simulation results. This chapter discusses this comparison.

## 2.2 Simulation parameter measurement system

### 2.2.1 Exposure equipment for parameter measurement

Fig.10 shows the exposure equipment used in our parameter measurements. The exposure area is an open-frame pattern measuring 10 mm x 10 mm. We used a UVES-2000 for KrF exposures and an EUVES-7000 [14] for EUV exposures.



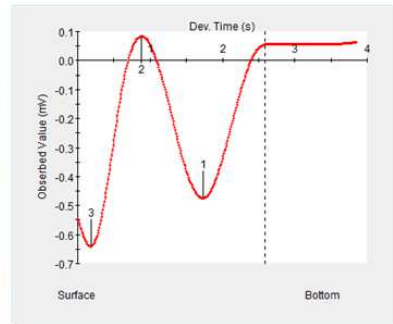
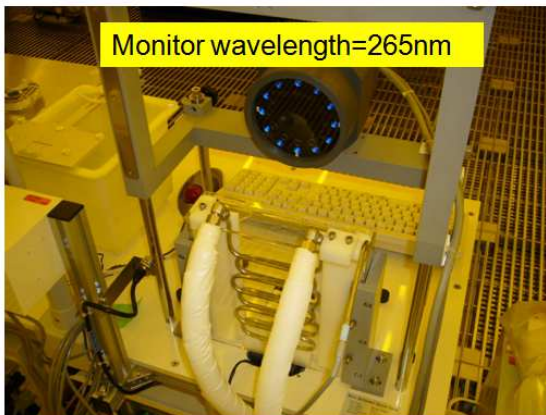
Fig. 10. Open frame exposure tool for KrF and EUV

These exposure tools permit resist exposures on Si wafers and the acquisition of development and PEB parameters.

### 2.2.2 Development parameter measurement system

We used a development analyzer to measure development parameters. When homogeneous light is irradiated onto a resist film during development, the light waves reflected from the resist surface and light waves reflected from the wafer surface interfere, generating unique waveforms. Analyzing the waveforms of the reflected light allows us to obtain resist development rates. By varying exposure values and measuring resist development rates at different exposures, we can calculate the development parameter, among the simulation parameters [15]. This measurement has been performed before using a monitor wavelength of 470 nm. However, thin films do not generate the interference needed, and a monitor wavelength of 470 nm limits us to resist film thicknesses exceeding 100 nm. Since the film thickness of EUV resists ranges from approximately 50 to 100 nm, we developed a measurement system for our experiments based on a monitor wavelength of 265 nm (Fig.11).

## Development parameter measurement system



MET-1K  
 Thickness=125nm  
 Exposure dose=5mJ/cm<sup>2</sup>  
 Wave data of RDA @ 265nm  
 monitor wavelength

Fig. 11. Resist development analyzer RDA-800EUV

### 2.2.3 B parameter measurement system

We used the following equation to calculate the B parameter [16-17] of Dill based the resist transmission factor at the time overexposure completely breaks down the PAG.

$$B = -\frac{1}{d} \ln(T_{\infty}) \quad (1)$$

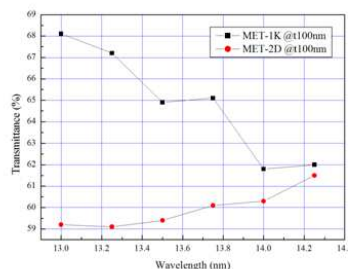
Here,  $d$  is resist film thickness and  $T_{\infty}$  the resist transmission factor at the time overexposure completely breaks down the PAG. We developed a system for measuring the resin transmission factor using EUV light. Incorporating a LPP light manufactured by Toyota Macs as its light source and using a solid Cu target, this system irradiates EUV light onto a Si/Mo multilayer reflecting mirror to measure reflection intensity, while mirror angles are varied. To calculate the spectral transmission factor, we used the difference in reflectance between the case in which resist is applied to the multilayer mirror and the case in which no resist is applied.

Fig.12 illustrates the measurement system and gives a chart of the results of spectral transmission factor calculations for the MET resist.

## B parameter measurement system



A reflectance measurement tool by laser plasma EUV light source



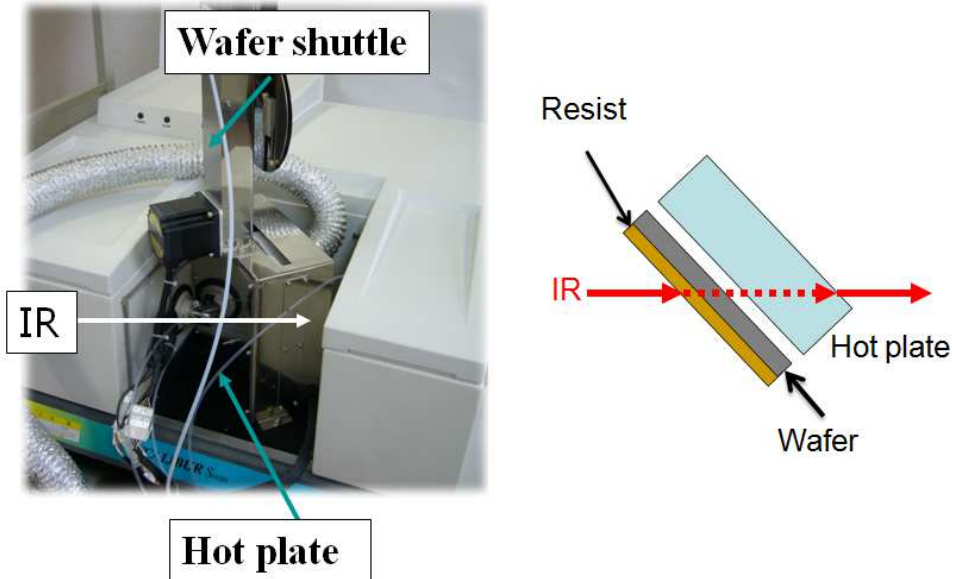
Light source: Laser plasma EUV source  
 Wavelength of light source : 2-20nm  
 Laser of excitation : YAG laser (523nm)  
 repetition frequency : 10Hz  
 Target : Cu  
 Output of EUV :  $2 \mu \text{W}/\text{cm}^2$

Fig. 12. B parameter measurement system using EUV exposure

### 2.2.4 De-protection reaction parameter and C parameter measurement system

Fig.13 gives an overview of the PEB parameter measurement system, which exposes resist on an Si wafer using KrF and EUV light. In the next step, we used an FT-IR system with a bake function to plot the de-protection reaction curve while performing PEB. We performed measurements at different PEB temperatures and measured the de-protection reaction parameter by fitting. During the course of fitting, we also obtained the C parameter for Dill. We modified the system [18] to allow irradiation of IR light for measurements on resist film at an angle of 45 degrees and to permit use with a resist film thickness of 50 nm. The resulting system was capable of handling extra-thin resist films ranging from 50 to 100 nm.

# PEB parameter measurement system



## De-protection reaction analysis system PAGA-100EUV

Fig. 13. PEB parameter measurement system

### 2.3 Parameter measurement results

We measured parameters using EUV chemically amplified resists MET-1K and MET-2D manufactured by Rohm and Haas.

Table 5 gives the process conditions.

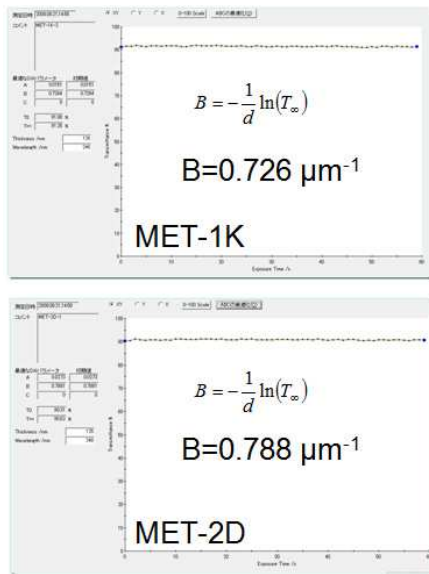
	Vendor	Thickness (nm)	PAB		PEB	
			Temp. (deg.C)	time (s)	Temp. (deg.C)	time (s)
MET-1K	R&H	125	130	60	110	90
MET-2D	R&H	125	130	60	110	90

R&H: Rohm and Haas

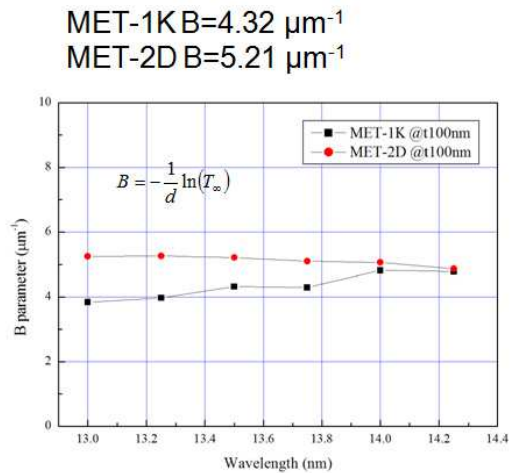
Table 5. Measurement conditions

### 2.3.1 B parameter measurement results

Fig.14 shows B parameter measurement results. With KrF exposures, MET-1K and MET-2D yielded values of 0.726 and 0.788, respectively. With EUV exposures, MET-1K and MET-2D yielded 4.32 and 5.21, respectively, indicating greater absorption with EUV exposures.



KrF(248nm) exposure



EUV(13.5nm) exposure

Fig. 14. B parameter measurement results

### 2.3.2 Development parameter measurement results

Fig.15 compares measurements of the discrimination curve (a logarithmic plot of development rates and exposure values) development parameter. We found no significant differences between development parameter values obtained with KrF and EUV exposures.

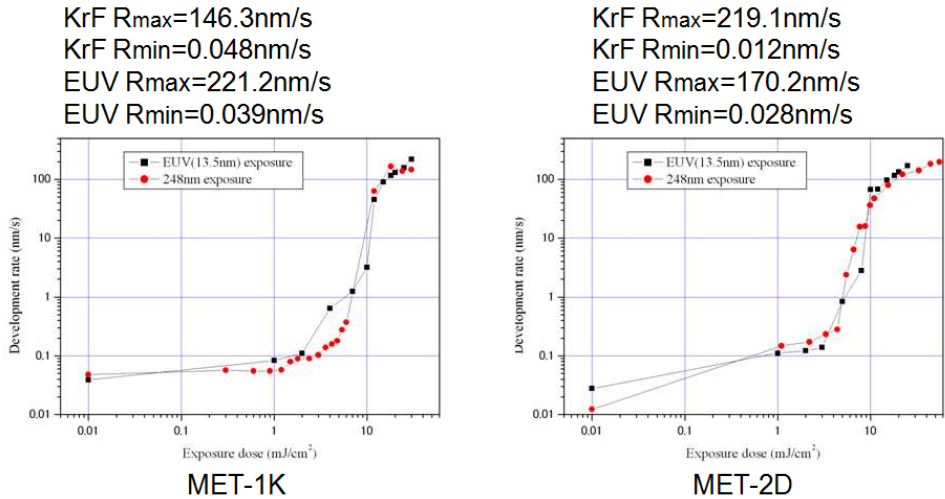
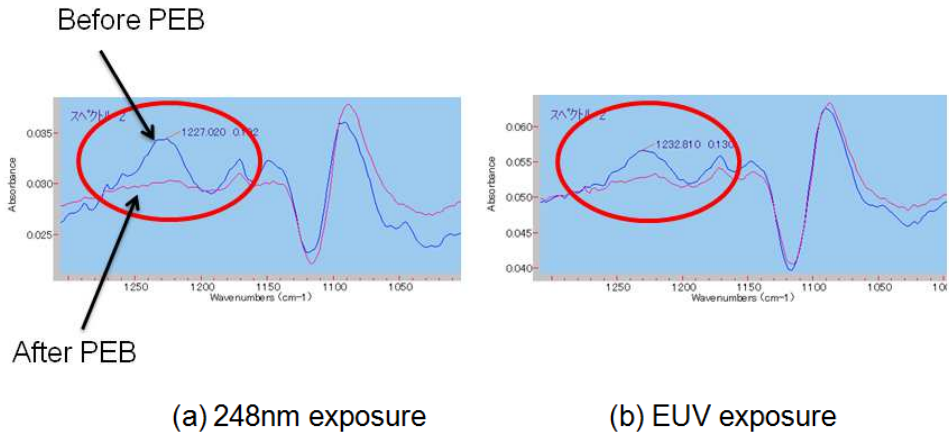


Fig. 15. Comparison of development parameter values

**2.3.3 De-protection reaction observations and results of de-protection reaction parameter measurements**

Fig.16 shows IR spectra obtained from the MET-1K before and after 16-mJ/cm<sup>2</sup> exposures. The figure indicates weakened (-CO) bonds due to de-protection reactions at 1,230 cm<sup>-1</sup>. The extent of the peak decline with KrF exposure is roughly identical to that with EUV, indicating the absence of significant differences in de-protection reactions.



**Comparison of light source and IR Spectra  
 MET-1K Resist@16mJ/cm<sup>2</sup>**

Fig. 16. Observations of de-protection reactions with KrF and EUV exposures



Table 6 is a list of simulation parameter measurement results.

	KrF(248nm) exposure		EUV(13.5nm) exposure	
	MET-1K	MET-2D	MET-1K	MET-2D
<b>ABC-parameter</b>				
A ( $1/\mu\text{m}$ )	0	0	0	0
B ( $1/\mu\text{m}$ )	0.726	0.788	4.32	5.21
C ( $\text{cm}^2/\text{mJ}$ )	0.017	0.021	0.086	0.090
<b>Development parameters (Mack original model)</b>				
Development $R_{\text{max}}$ (nm/s)	146.3	219.1	221.2	170.2
Development $R_{\text{min}}$ (nm/s)	0.048	0.012	0.039	0.028
Development $M_{\text{th}}$	0.773	0.783	0.624	0.518
Development n	15.21	17.30	12.65	18.96
<b>PEB parameters</b>				
PEB Amplification $E_a$ (Kcal/mol)	12.21	11.30	3.82	2.23
PEB Amplification $\text{LN}(\text{Ar})$ (1/s)	14.89	13.65	5.53	3.55
PEB Diffusion-Controlled Reaction $E_a$ (Kcal/mol)	8.56	4.82	8.80	1.00
PEB Diffusion-Controlled Reaction $\text{LN}(\text{Ar})$ (1/s)	10.14	5.54	11.50	1.78
PEB Diffusivity $E_a$ (Kcal/mol)	5.00	5.00	5.00	5.00
PEB Diffusivity $\text{LN}(\text{Ar})$ ( $\text{nm}^2/\text{s}$ )	23.22	21.24	30.00	30.00

Table 6. Simulation parameter measurement results

### 2.3.4 Examination of simulation

We performed EUVL simulations using the simulation parameters obtained. Table 7 gives the simulation conditions used.

#### Simulation condition

NA=0.30

Wavelength=13.5nm

Illumination= Annular (0.3/0.7)

Flare=1%

Line and space=28nm

Resist: MET-1K and MET-2D

Thickness:125nm

Table 7. Simulation conditions

For exposure equipment, our simulation assumed use of the Nikon EUV-1 installed at Selete [19]. Fig.17 shows the simulation results. The indicated exposure value is the exposure level ( $E_0$ ) that achieved 1:1 resolution from a 28-nm L&S pattern. The development conditions called for 2.38% TMAH and development time of 60 seconds. The quencher diffusion length and PAG diffusion length were set to 20 nm and 10 nm, respectively.

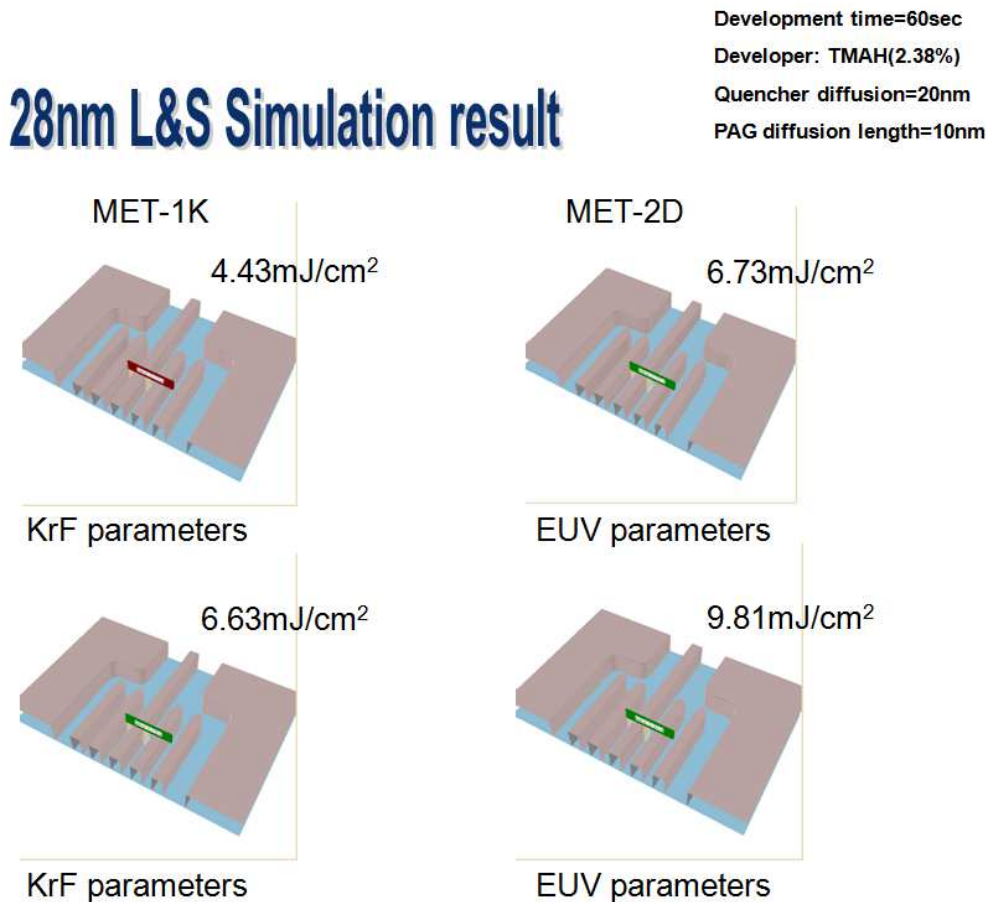


Fig. 17. Simulation results

We compared the results of EUVL simulations based on parameters obtained with KrF exposures to the results of EUVL simulations based on parameters obtained with EUV exposures. While the former simulation results indicated higher sensitivity (approximately 20% higher), we saw no major differences in shape.

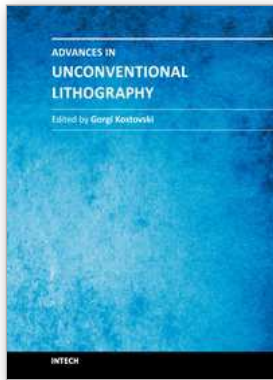
## 2.4 Conclusion

We compared the results of EUVL simulations based on parameters obtained with KrF exposures to the results of EUVL simulations based on parameters obtained with EUV exposures. The former resulted in approximately 20% higher simulation sensitivity, but we saw no major differences in shape. Using parameters obtained with KrF exposure is a roundabout way to perform EUVL simulations. Since EUV exposures in many cases are not readily available, a valid option would appear to be to acquire simulation parameters through KrF exposures and to use these parameters as initial values in calculations for EUVL simulations.

## 3. References

- [1] B. J. Lin, *Proc. SPIE*, 4688, 11, 2002
- [2] IMEC 4th Immersion Workshop, September in Belgium, 2005
- [3] V. N. Golovkina, P. F. Nealy, F. Cerrina, J. W. Taylor, H. H. Saolak, C. David and J. Gobrecht, *J. Vac. Sci., Technol. B*, 22(1), 99, 2004
- [4] Intel H.P.  
<http://www.intel.com/jp/technology/index.htm?iid=subhdr-JP+tech>
- [5] ITRS 2005 : International Technology Roadmap for Semiconductors 2005 Edition
- [6] H. B. Cao, W. Yueh, J. Roberts, B. Rice, R. Bristol and M. Chandhok. *Proc. SPIE*, 5753, 459, 2005
- [7] NIKON H.P.  
[http://www.nikon.co.jp/news/2007/0711\\_nsr\\_01.htm](http://www.nikon.co.jp/news/2007/0711_nsr_01.htm)
- [8] ASLM H.P.  
URL : <http://www.asml.co.jp>
- [9] P. Blackborow, *Proc. SPIE*, 6151, 25, 2006
- [10] A. Sekiguchi, C. A. Mack, Y. Minami and T. Matsuzawa, *Proc. SPIE*, 2725, 49, 1996
- [11] Prolith Version 9.3 User's manual
- [12] ITRS LOAD MAP 2007 Up-date in Web
- [13] 7<sup>th</sup> EUVL symposium in Lake Tahoe, CA (2008.10)
- [14] A. Sekiguchi, Y. Kono, M. kadoi, Y. Minami, T. Kozawa, S. Tagawa, D. Gustafson and P. Blackborow, *Proc. SPIE*, 6519, 168 (2007).
- [15] A. Sekiguchi, Y. Minami, and Y. Sensu, The Electrochemical Society of Japan, Proc. of the 42<sup>nd</sup> Sysmp. on Semiconductors and Integrated Circuits Technology, Vol. 42, pp. 109-114 (1992).
- [16] Dill-B F. H. Dill, W. P. Hornberger, P. S. Hauge, and J. M. Shaw, *IEEE Trans. Electron Dev.*, Vol. ED-22, No. 7, pp. 445-452 (1975).
- [17] C. A. Mack, T. Matsuzawa, A. Sekiguchi, and Y. Minami, *Proc. SPIE*, Vol. 2725, pp. 34-48 (1996).

- [18] A. Sekiguchi, and Y. Kono, *Proc. SPIE*, 6923, 92 (2008)
- [19] H. Oizumi, D. Kawamura, K. Kaneyama, S. Kobayashi and T. Itani, RE-03, 7<sup>th</sup> EUVL symposium (2008).



## **Advances in Unconventional Lithography**

Edited by Dr. Gorgi Kostovski

ISBN 978-953-307-607-2

Hard cover, 186 pages

**Publisher** InTech

**Published online** 09, November, 2011

**Published in print edition** November, 2011

The term Lithography encompasses a range of contemporary technologies for micro and nano scale fabrication. Originally driven by the evolution of the semiconductor industry, lithography has grown from its optical origins to demonstrate increasingly fine resolution and to permeate fields as diverse as photonics and biology. Today, greater flexibility and affordability are demanded from lithography more than ever before. Diverse needs across many disciplines have produced a multitude of innovative new lithography techniques. This book, which is the final instalment in a series of three, provides a compelling overview of some of the recent advances in lithography, as recounted by the researchers themselves. Topics discussed include nanoimprinting for plasmonic biosensing, soft lithography for neurobiology and stem cell differentiation, colloidal substrates for two-tier self-assembled nanostructures, tuneable diffractive elements using photochromic polymers, and extreme-UV lithography.

### **How to reference**

In order to correctly reference this scholarly work, feel free to copy and paste the following:

Atsushi Sekiguchi (2011). Approach to EUV Lithography Simulation, Advances in Unconventional Lithography, Dr. Gorgi Kostovski (Ed.), ISBN: 978-953-307-607-2, InTech, Available from:  
<http://www.intechopen.com/books/advances-in-unconventional-lithography/approach-to-euv-lithography-simulation>

**INTECH**  
open science | open minds

### **InTech Europe**

University Campus STeP Ri  
Slavka Krautzeka 83/A  
51000 Rijeka, Croatia  
Phone: +385 (51) 770 447  
Fax: +385 (51) 686 166  
[www.intechopen.com](http://www.intechopen.com)

### **InTech China**

Unit 405, Office Block, Hotel Equatorial Shanghai  
No.65, Yan An Road (West), Shanghai, 200040, China  
中国上海市延安西路65号上海国际贵都大饭店办公楼405单元  
Phone: +86-21-62489820  
Fax: +86-21-62489821

© 2011 The Author(s). Licensee IntechOpen. This is an open access article distributed under the terms of the [Creative Commons Attribution 3.0 License](#), which permits unrestricted use, distribution, and reproduction in any medium, provided the original work is properly cited.